

## Supporting Information

for *Adv. Sci.*, DOI 10.1002/adv.202203718

STING Suppresses Mitochondrial VDAC2 to Govern RCC Growth Independent of Innate Immunity

*Zhichuan Zhu, Xin Zhou, Hongwei Du, Erica W. Cloer, Jiaming Zhang, Liu Mei, Ying Wang, Xianming Tan, Austin J. Hepperla, Jeremy M. Simon, Jeanette Gowen Cook, Michael B. Major, Gianpietro Dotti and Pengda Liu\**

## Supporting Information for

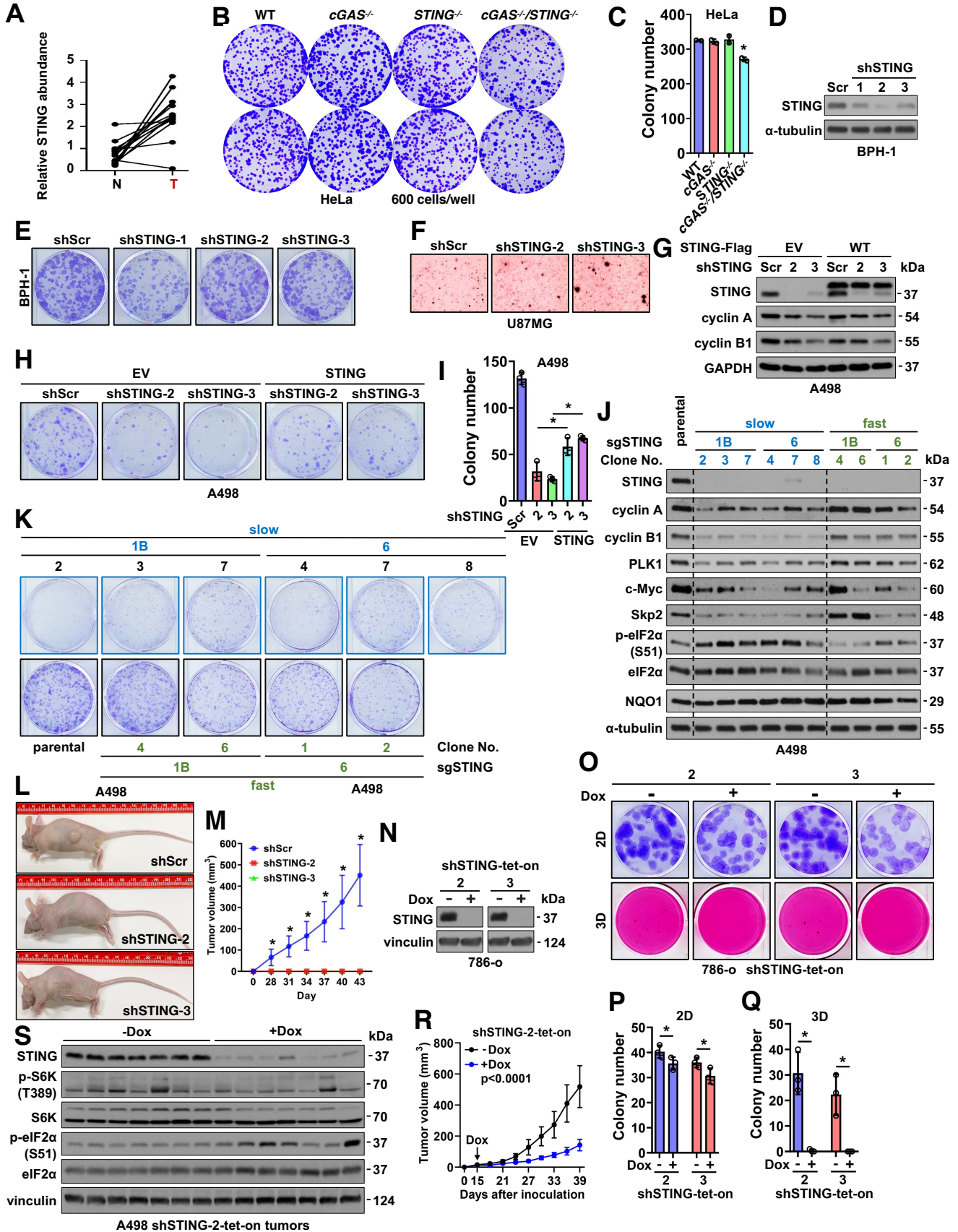
### **STING suppresses mitochondrial VDAC2 to govern RCC growth independent of innate immunity**

Zhichuan Zhu, Xin Zhou, Hongwei Du, Erica W. Cloer, Jiaming Zhang, Liu Mei, Ying Wang, Xianming Tan, Austin J. Hepperla, Jeremy M. Simon, Jeanette Gowen Cook, Michael B. Major, Gianpietro Dotti and Pengda Liu

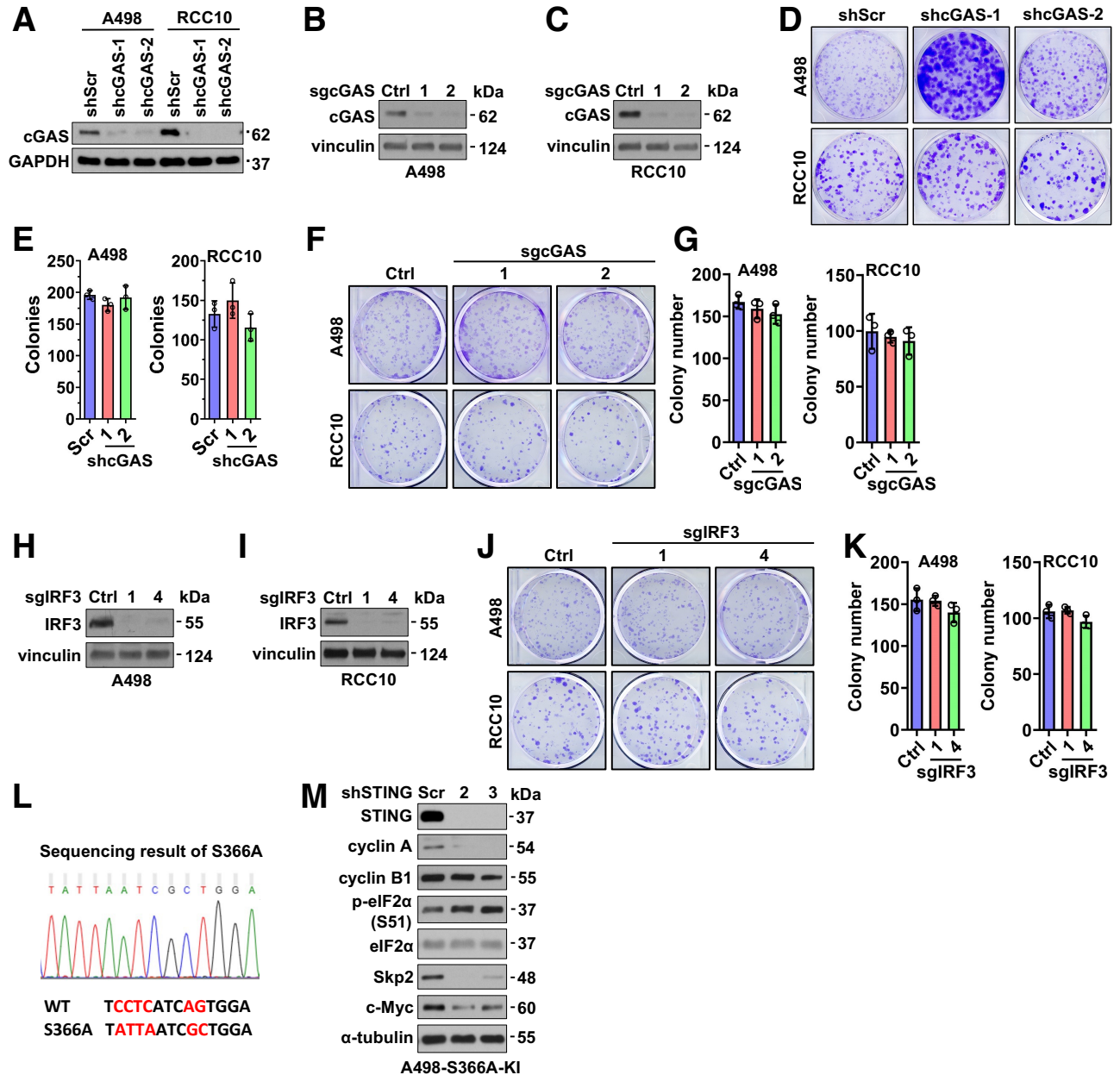
correspondence to: [pengda\\_liu@med.unc.edu](mailto:pengda_liu@med.unc.edu)

**This PDF file includes:**

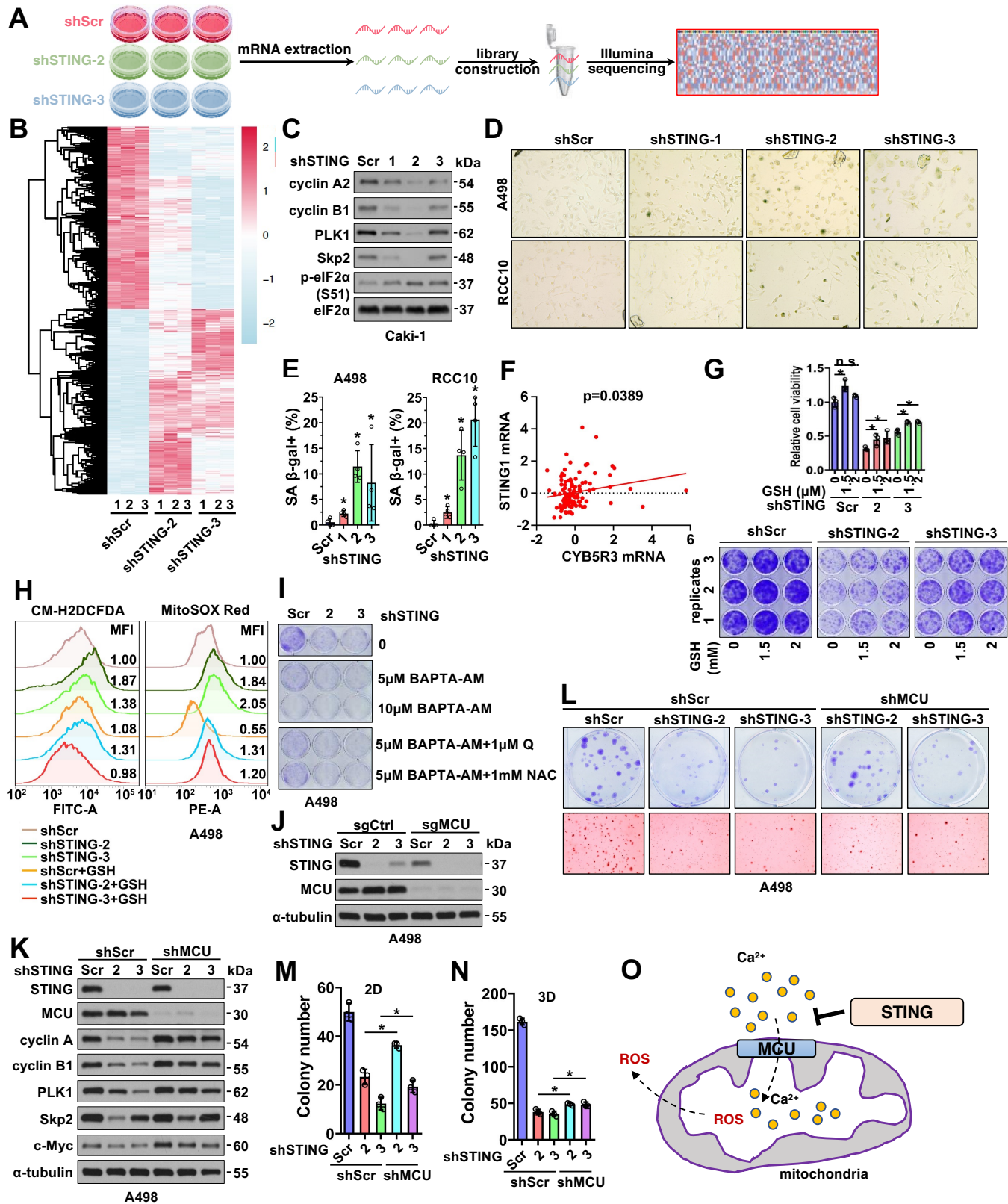
Figs. S1 to S9



**Figure S1. STING depletion reduces RCC cell growth.** (A) A quantification of Fig. 1C. (B) Representative images for 2D colony formation assays using indicated HeLa cells and quantified in (C). Error bars were calculated as mean $\pm$ -SD, n=3. \*p < 0.05 (one-way ANOVA test). (D) IB analyses of WCL from indicated BPH-1 cells. (E) Representative images for 2D colony formation assays using BPH-1 cells obtained in (D). (F) Representative images for 3D silt agar growth assays using indicated U87MG cells. (G) IB analyses of WCL from indicated A498 cells. Where indicated, WT-STING was stably expressed in A498 cells by lentiviral infection, followed by infection with control or STING shRNA containing viruses to deplete endogenous STING. (H) Representative images for 2D colony formation assays using A498 cells obtained in (G) and quantified in (I). Error bars were calculated as mean $\pm$ -SD, n=3. \*p < 0.05 (one-way ANOVA test). (J) IB analyses of WCL from indicated A498 single clones from infection with sgRNAs against endogenous STING. (K) Representative images for 2D colony formation assays using A498 cells obtained in (J). (L) Representative images for nude mice injected with indicated A498 cells. (M) Tumor volume measurements at indicated days post-injection of indicated A498 cells. Error bars were calculated as mean $\pm$ -SD, n=8. \*p < 0.05 (one-way ANOVA test). (N) IB analyses of WCL from A498 or RCC10 cells depleted of endogenous cGAS. (O) Representative images of 2D colony formation assays using cells obtained in (N) and quantified in (P and Q). Error bars were calculated as mean $\pm$ -SD, n=3. \*p < 0.05 (one-way ANOVA test). (R) Tumor volume measurements at indicated days post-injection of indicated A498 cells. Error bars were calculated as mean $\pm$ -SD, n=8. \*p < 0.05 (one-way ANOVA test). (S) IB analysis of WCL derived from indicated A498 tumors from (R).



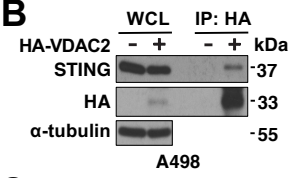
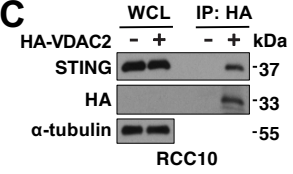
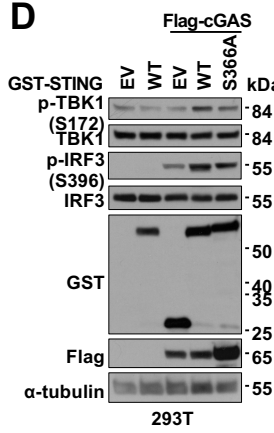
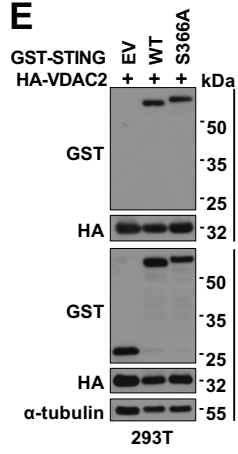
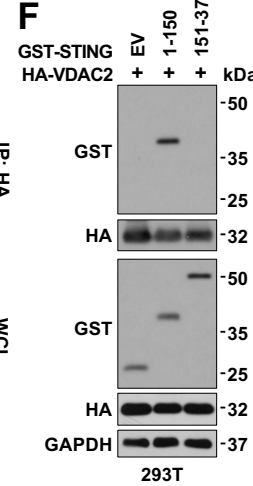
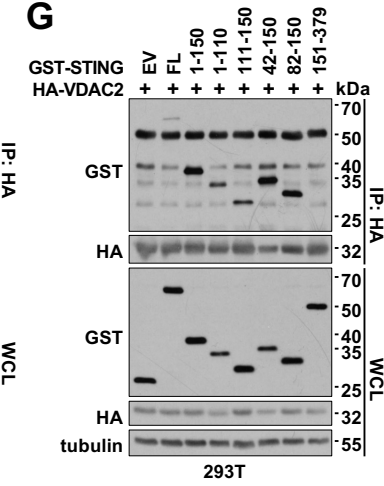
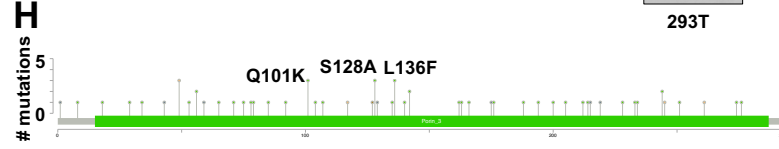
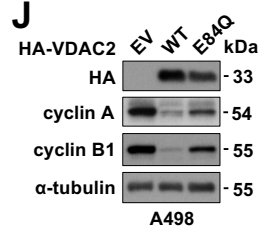
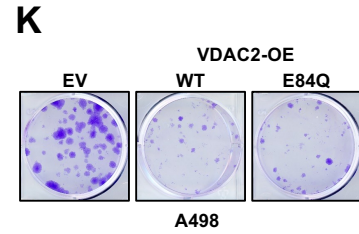
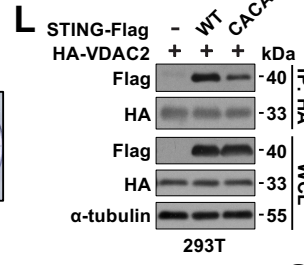
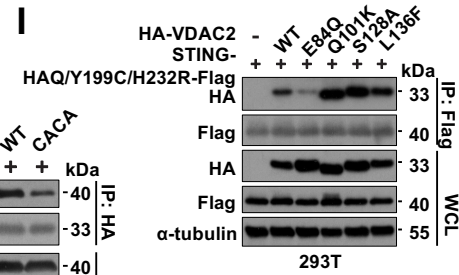
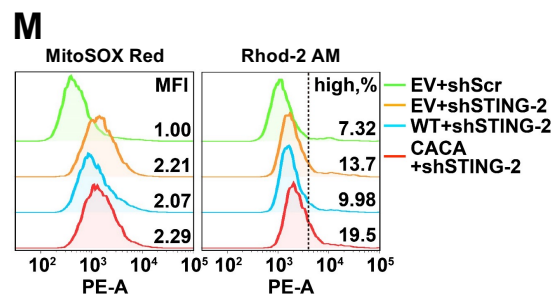
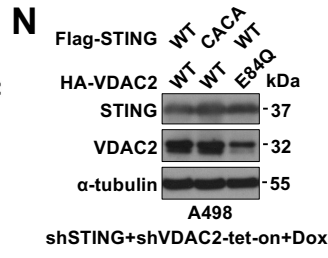
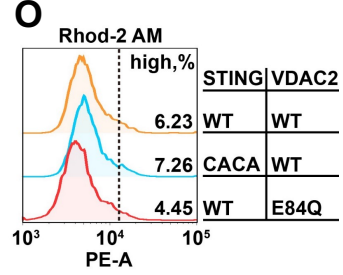
**Figure S2. STING depletion reduces RCC cell growth independent of STING's innate immunity function.** (A, B, C) IB analysis of WCL derived from indicated cGAS depleted A498 and RCC10 cells. (D, F) Representative images of 2D colony formation assays using cells obtained in (A-C) and quantified in (E, G). Error bars were calculated as mean $\pm$ SD, n=3. \*p < 0.05 (one-way ANOVA test). (H, I) IB analysis of WCL derived from indicated cGAS depleted A498 and RCC10 cells. (J) Representative images of 2D colony formation assays using cells obtained in (H, I) and quantified in (K). Error bars were calculated as mean $\pm$ SD, n=3. \*p < 0.05 (one-way ANOVA test). (L) DNA sanger sequencing result to validate the STING-S366A knockin A498 clones. (M) IB analysis of WCL from indicated A498-S366A knockin cells.



**Figure S3. STING depletion in A498 cells leads to deregulation in cell cycle progression caused by imbalance in mitochondrial calcium homeostasis.** (A) A cartoon illustration for the pipeline for RNA-Seq. (B) A heatmap to summarize changes of genes in redox homeostasis (redox gene set in Harmonizome database) in control or STING depleted A498 cells from RNA-Seq. (C) IB analyses of WCL derived from indicated Caki-1 cells. (D) Representative images for  $\beta$ -galactosidase staining using cells from D and quantified in E. Error bars were calculated as mean $\pm$ -SD, n=3. \*p<0.05 (one-way ANOVA test). (F) mRNA expression of STING1 positively correlates with CYB5R3 analyzed using CPTAC data from [1]. (G) Representative images for 2D colony formation assays using indicated A498 cells treated with indicated doses of GSH. Where indicated, GSH treatment was refreshed every other day for 9 days and quantified by measuring OD590 of resolved crystal violet in 10% acetic acid solution. Error bars were calculated as mean $\pm$ -SD, n=3. \*p < 0.05 (one-way ANOVA test). (H) FACS analyses of cellular ROS levels and mitochondrial ROS levels with indicated treated in indicated A498 cells. (I) Representative images for 2D colony formation assays using indicated A498 cells treated with indicated doses of compounds. Where indicated, BAPTA-AM treatment was refreshed every other day for 7 days. (J, K) IB analyses of WCL derived from indicated A498 cells. (L) Representative images for both 2D colony formation assays and 3D soft agar assays using cells generated in (K) and quantified in (M) and (N). Error bars were calculated as mean $\pm$ -SD, n=3. \*p < 0.05 (one-way ANOVA test). (O) A cartoon illustration showing that STING suppresses calcium transport into mitochondria such that MCU depletion rescues STING depletion induced mitochondria calcium and ROS increases.

**A**

Enrichment FDR	Genes in list	Total genes	Functional Category
9.8E-78	78	149	Protein localization to ER
<b>5.3E-76</b>	<b>69</b>	<b>111</b>	<b>Selective membrane channel proteins</b>
1.3E-74	67	106	SRP-dependent cotranslational protein targeting to membrane
3.6E-73	70	124	Establishment of protein localization to ER
3.0E-71	68	120	Protein targeting to ER
1.8E-63	78	212	Translational initiation

**B****C****D****E****F****G****H****J****K****L****I****M****N****O**



**Figure S4. STING binds VDAC2 to regulate mitochondrial calcium homeostasis.** (A) Functional analyses of statistically significant STING binding partners. (B, C) IB analyses of HA-IP (right panel) and WCL (left panel) from A498 (B) or RCC10 (C) cells. (D) IB analyses of WCL from HEK293T cells transfected with indicated DNA constructs. (E, F, G) IB analyses of HA-IP and WCL from HEK293T cells transfected with indicated DNA constructs. (H) An illustration of most frequently observed VDAC2 cancer patient derived mutations (from cbiportal). (I) IB analyses of Flag-IP and WCL derived from HEK293T cells transfected with indicated VDAC2 and STING constructs. (J) IB analyses of WCL from A498 cells stably expressing indicated lentiviral HA-VDAC2 constructs. (K) Representative images for 2D colony formation assays using cells obtained from (J). (L) IB analyses of HA-IP and WCL from HEK293T cells transfected with HA-VDAC2 and indicated STING constructs. (M) FACS analyses of mitochondrial ROS (MitoSOX Red) or mitochondrial calcium (Rhod-2 AM) in indicated A498 cells. (N) IB analyses of WCL from iSTING/VDAC2 double depleted A498 cells expressing indicated STING and VDAC2. (O) FACS analyses of mitochondrial calcium (Rhod-2 AM) in indicated A498 cells from N.

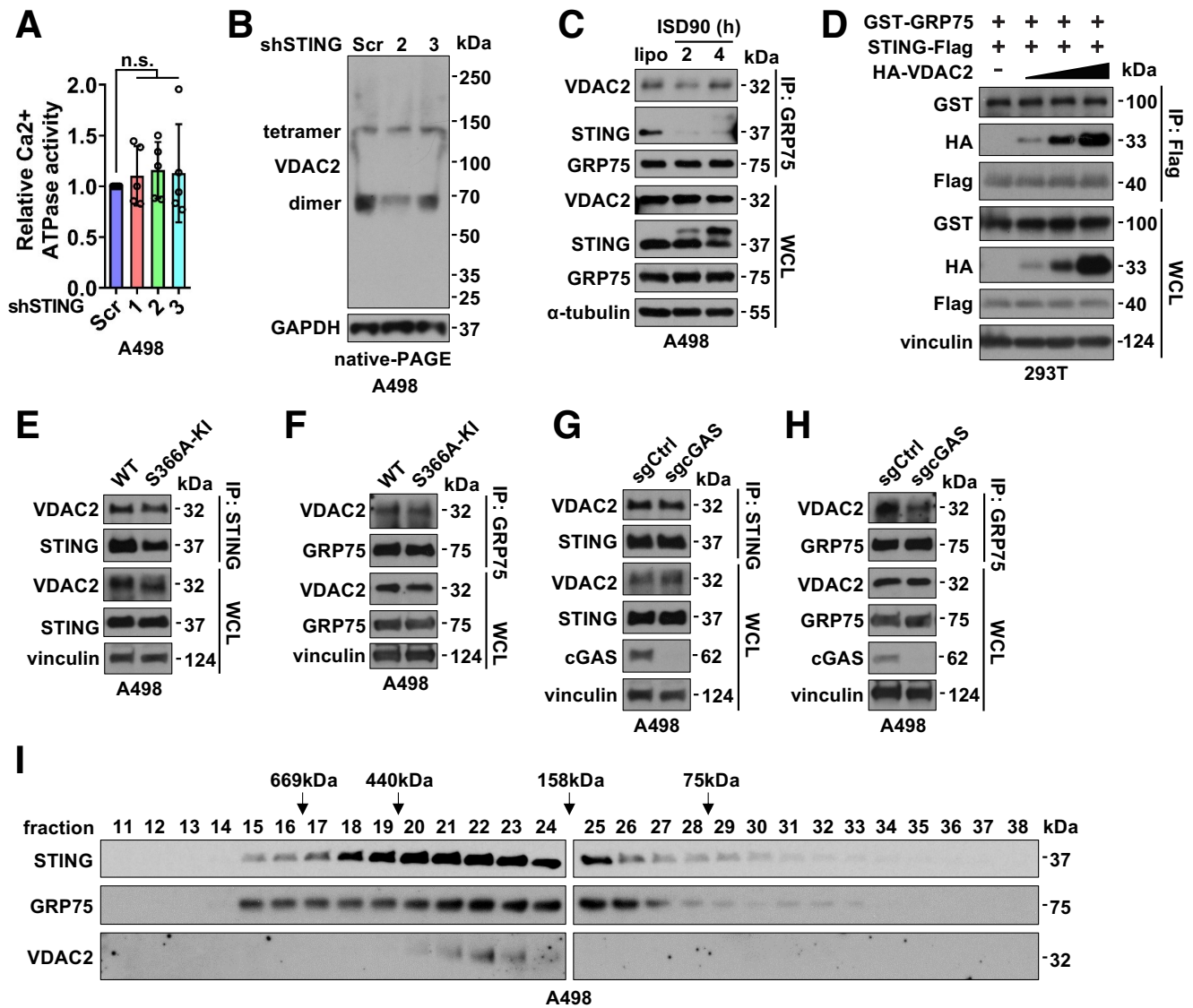


**Figure S5. STING depletion does not affect VDAC2 oligomerization but interferes with MERC.** (A) A Ca<sup>2+</sup> related ATPase activity assay using indicated A498 cell lysates. Activity was measured using a Ca<sup>2+</sup> ATPase activity assay kit (Elabscience) according to manufacturer's protocol. Error bars were calculated as mean $\pm$ SD, n=5. n.s., no significance (one-way ANOVA test). (B) IB analyses of WCL in indicated STING depleted A498 cells using native PAGE. (C) IB analyses of GRP75-IP and WCL from A498 cells treated with lipofectamine 3000 or ISD90 (5  $\mu$ g/mL) for indicated hrs before cell collection. (D) IB analyses of Flag-IP and WCL derived from HEK293T cells transfected with indicated DNA constructs. (E, G) IB analyses of STING-IP and WCL derived from indicated A498 cells. (F, H) IB analyses of GRP75-IP and WCL derived from indicated A498 cells. (I) IB analyses of FPLC fractions using A498 cell lysates.

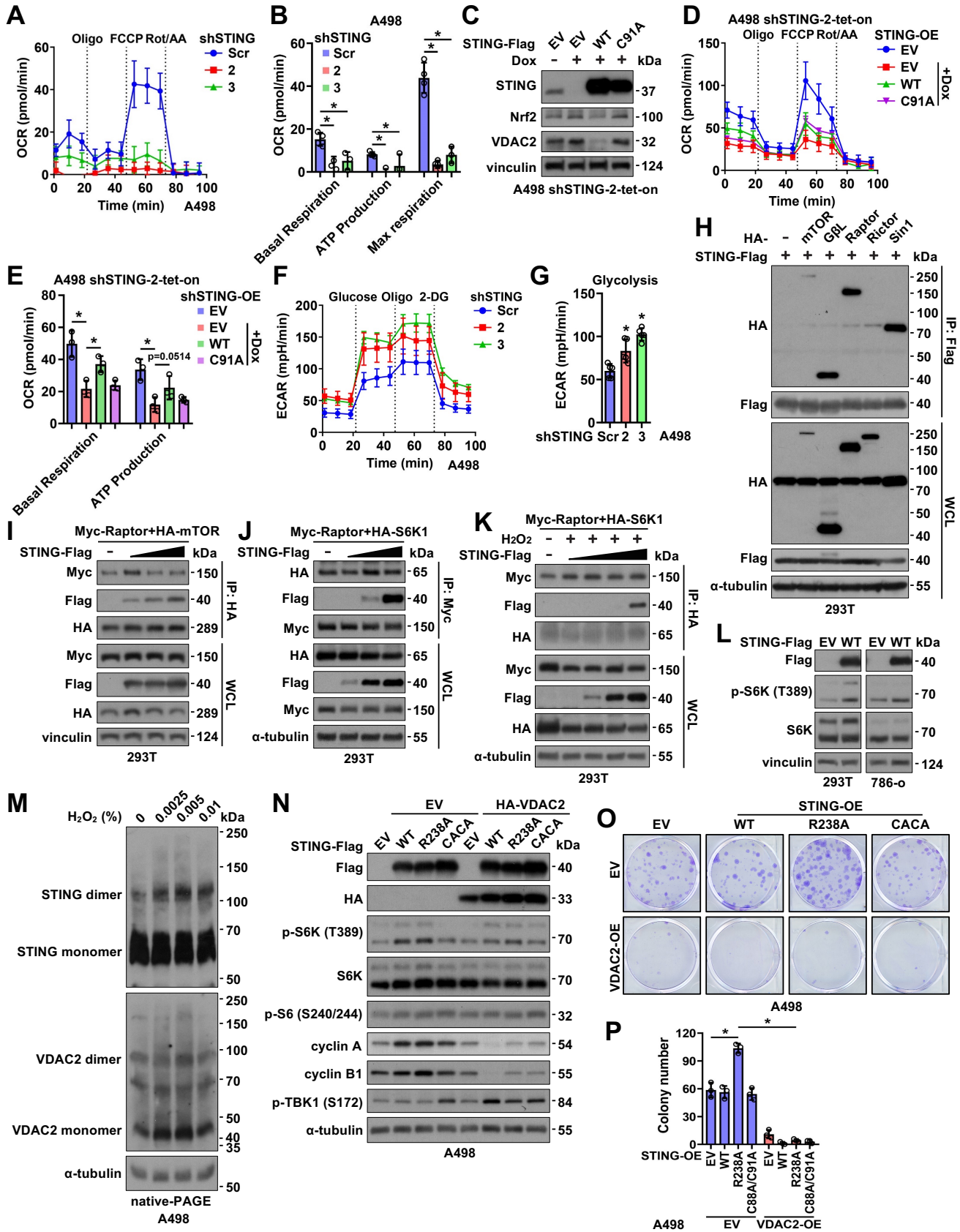


**Figure S6. STING depletion attenuates mitochondria function and suppresses mTORC1/S6K signaling to inhibit RCC cell growth.** (A) Normalized OCR plots using indicated shSTING A498 cells. Quantifications are shown in (B). Error bars were calculated as mean $\pm$ -SD, n=4. \*p<0.05 (one-way ANOVA test). (C) IB analysis of WCL from indicated A498-tet-on-shSTING cells. (D) Normalized OCR plots using shSTING-tet-on A498 cells treated with or without 1 mg/mL doxycycline treatment for 4 days. Quantifications are shown in (E). Error bars were calculated as mean $\pm$ -SD, n=3. \*p<0.05 (one-way ANOVA test) (F) Normalized ECAR plots using indicated shSTING A498 cells. Quantifications are shown in (G). Error bars were calculated as mean $\pm$ -SD, n=5. \*p<0.05 (one-way ANOVA test). (H) IB analyses of Flag-IP and WCL derived from HEK293T cells transfected with indicated HA constructs with Flag-STING. (I) IB analyses of HA-IP and WCL derived from HEK293T cells transfected with indicated doses of Flag-STING with Myc-Raptor and HA-mTOR. (J) IB analyses of Myc-IP and WCL derived from HEK293T cells transfected with indicated doses of Flag-STING with Myc-Raptor and HA-S6K1. (K) IB analyses of HA-IP and WCL derived from HEK293T cells transfected with indicated doses of Flag-STING with Myc-Raptor and HA-S6K1 treated with 0.01% H<sub>2</sub>O<sub>2</sub> for 6 hrs before cell collection. (L) IB analyses of WCL from HEK293T cells transfected with indicated DNA constructs or 786-o cells infected with indicated lenti-viruses. (M) IB analyses of WCL from A498 cells treated with indicated doses of H<sub>2</sub>O<sub>2</sub>. (N) IB analyses of WCL from A498 cells stably expressing indicated STING-Flag and HA-VDAC2 by lentiviral infection. (O) Representative of 2D colony formation images for cells obtained in (M) and quantified in (P). Error bars were calculated as mean $\pm$ -SD, n=3. \*p<0.05 (one-way ANOVA test).

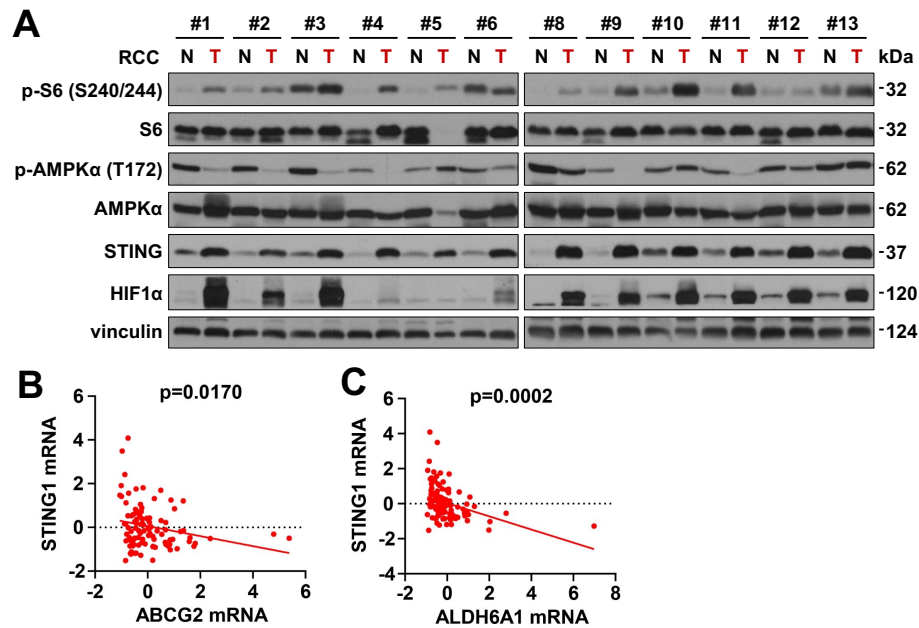


**Figure S7. Increased mTORC1 signaling was observed in RCC patient tissues.** (A) IB analyses of WCL from 12 pairs of RCC tumor tissues with matched normal adjacent tissues. (B, C) STING mRNA is inversely correlated with expression of NRF2 targets ABCG2 and ALDH6A1 in CPTAC data from [1].

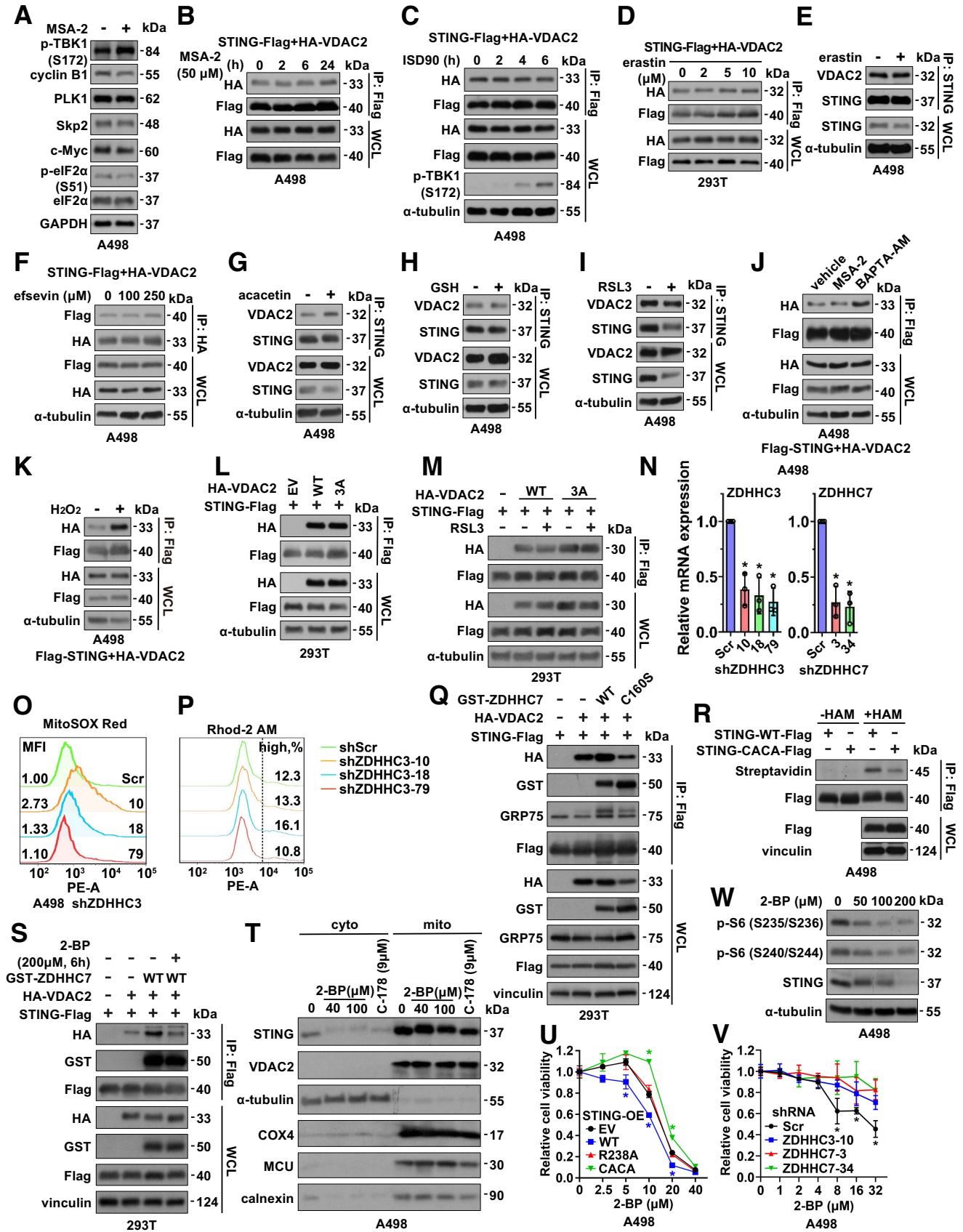


**Figure S8. Disrupting STING binding to VDAC2 reduces RCC growth.** (A) IB analyses of WCL from A498 cells treated with or without 50  $\mu$ M MSA-2 for 24 hrs before cell collection. (B, C) IB analyses of Flag-IP and WCL from A498 cells stably expressing Flag-STING and HA-VDAC2 by lentiviral infection treated with 50  $\mu$ M MSA-2 (B) or 5  $\mu$ g/ml ISD90 (C) for indicated time periods. (D) IB analyses of Flag-IP and WCL from HEK293T cells transfected with Flag-STING and HA-VDAC2 treated with indicated doses of erastin for 24 hrs prior to cell collection. (E) IB analyses of STING-IP and WCL from A498 cells treated with 5  $\mu$ M erastin for 24 hrs prior to cell collection. (F) IB analyses of HA-IP and WCL from A498 cells stably expressing Flag-STING and HA-VDAC2 treated with indicated doses of efsevin for 24 hrs prior to cell collection. (G, H, I) IB analyses of STING-IP and WCL from A498 cells treated with 1  $\mu$ M acacetin (G), 6 mM GSH (H), 0.5  $\mu$ M RSL3 (I) for 24 hrs prior to cell collection. (J) IB analyses of Flag-IP and WCL from A498 cells stably expressing Flag-STING and HA-VDAC2 by lentiviral infection treated with 50  $\mu$ M MSA-2 or 10  $\mu$ M BAPTA-AM for 24 hrs prior to cell collection. (K) IB analyses of Flag-IP and WCL from A498 cells stably expressing Flag-STING and HA-VDAC2 by lentiviral infection treated with 0.1% H<sub>2</sub>O<sub>2</sub> for 1 hr prior to cell collection. (L) IB analyses of Flag-IP and WCL derived from HEK293T cells transfected with indicated DNA constructs. (M) IB analyses of Flag-IP and WCL derived from HEK293T cells transfected with indicated DNA constructs and treated with 0.5  $\mu$ M RSL3 for 3 hrs prior to cell collection. (N) RT-PCR analyses of indicated ZDHHC mRNAs to examine indicated ZDHHC knockdown efficiency. Error bars were calculated as mean $\pm$ SD, n=3. \*p<0.05 (one-way ANOVA test). (O) FACS analyses of mitochondria ROS (MitoSOX Red) in indicated A498 cells. (P) FACS analyses of mitochondria calcium (Rhod-2 AM) in indicated A498 cells. (Q) IB analyses of Flag-IP and WCL derived from HEK293T cells transfected with indicated DNA constructs. (R) IB analyses of Flag-IP and WCL derived from A498 cells overexpressing STING-WT and -CACA. (S) IB analysis of indicated fractions from A498 cells treated with indicated compounds for 24 hrs. (T) IB analysis of WCL from A498 cells treated with indicated doses of 2-BP overnight before cell collection. (U, V) Analyses of relative viability of indicated A498 cells treated with indicated doses of 2-BP for 4 days before cell viability is measured. Error bars were calculated as mean $\pm$ SD, n=3.

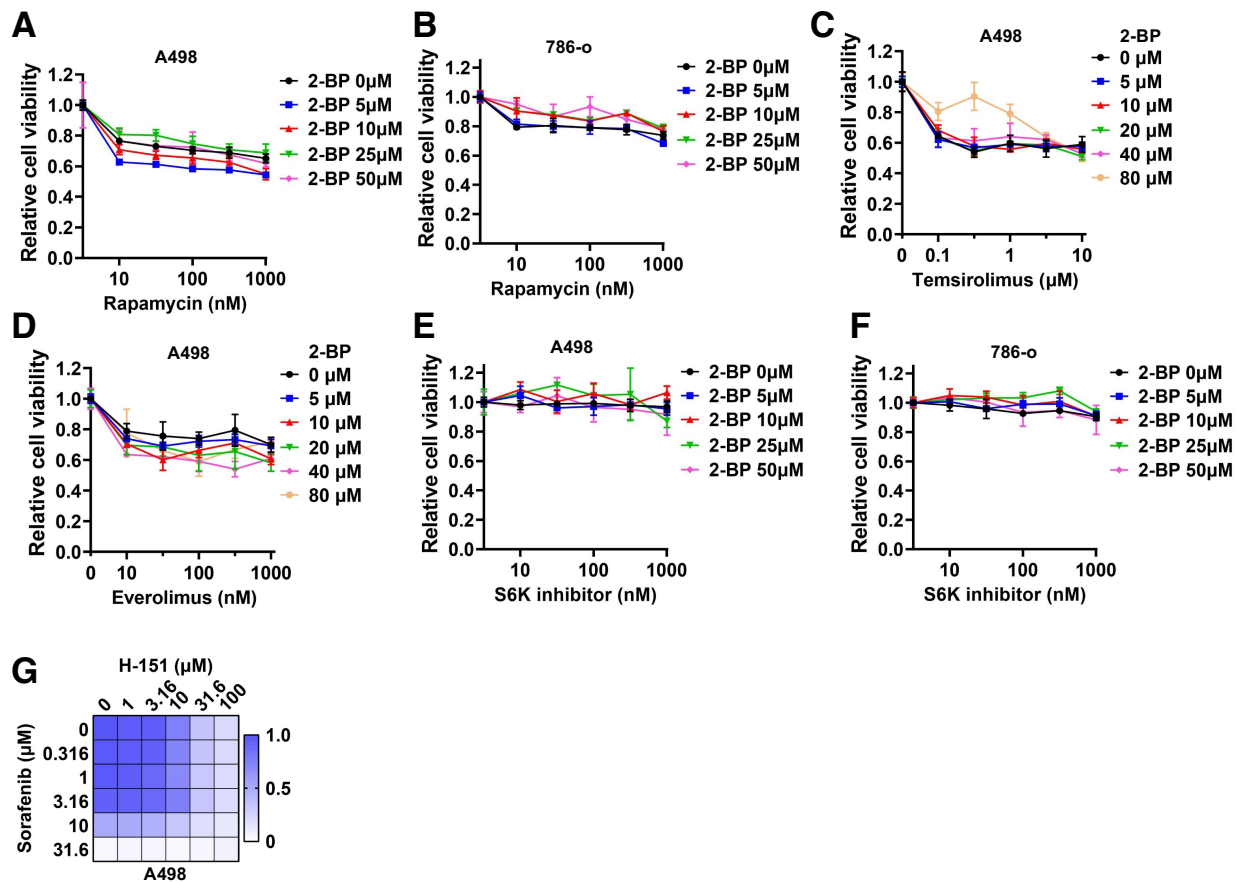


**Figure S9. 2-BP and sorafenib displays a synergy in suppressing A498 tumor growth.** (A-F) Analyses of relative viability of indicated RCC cells treated with indicated doses of 2-BP and indicated compounds for 2 days before cell viability is measured. Error bars were calculated as mean $\pm$ SD, n=3. (G) A representative heatmap for viability of A498 cells treated with indicated doses of compounds for 4 days.



**References:**

1. Clark, D.J., Dhanasekaran, S.M., Petralia, F., Pan, J., Song, X., Hu, Y., da Veiga Leprevost, F., Reva, B., Lih, T.M., Chang, H.Y., *et al.* (2019). Integrated Proteogenomic Characterization of Clear Cell Renal Cell Carcinoma. *Cell* 179, 964-983 e931.